

RAPID COMMUNICATION

Disruption of Ripple-Associated Hippocampal Activity During Rest Impairs Spatial Learning in the Rat

Valérie Ego-Stengel* and Matthew A. Wilson

ABSTRACT: The hippocampus plays a key role in the acquisition of new memories for places and events. Evidence suggests that the consolidation of these memories is enhanced during sleep. At the neuronal level, reactivation of awake experience in the hippocampus during sharp-wave ripple events, characteristic of slow-wave sleep, has been proposed as a neural mechanism for sleep-dependent memory consolidation. However, a causal relation between sleep reactivation and memory consolidation has not been established. Here we show that disrupting neuronal activity during ripple events impairs spatial learning. We trained rats daily in two identical spatial navigation tasks followed each by a 1-hour rest period. After one of the tasks, stimulation of hippocampal afferents selectively disrupted neuronal activity associated with ripple events without changing the sleep-wake structure. Rats learned the control task significantly faster than the task followed by rest stimulation, indicating that interfering with hippocampal processing during sleep led to decreased learning. © 2009 Wiley-Liss, Inc.

KEY WORDS: memory; consolidation; microstimulation; sharp-wave ripple events; CA1

INTRODUCTION

The medial temporal lobe has long been recognized to be a key structure for the acquisition and consolidation of memories for facts and events (Squire et al., 2004). In the rat, spatial memory in particular depends heavily on the integrity of the hippocampus. In 1989, Buzsáki proposed an influential model identifying two main stages in memory formation, each associated with specific network activity patterns (Buzsáki, 1989). The initial encoding of a new spatial environment would result from the integration of information coming from the neocortex

by the hippocampal network, and this would be favored by the exploratory theta rhythm (around 8 Hz). After behavior, the high recurrent excitation during population bursts (Buzsáki, 1986) would promote the transfer of information back to the neocortex, leading to a long-term memory storage largely independent from the hippocampus (Kali and Dayan, 2004). In this framework, the consolidation stage depends heavily on population bursts, commonly referred to as sharp wave-ripple events in CA1.

Sharp wave-ripple events occur mainly during slow-wave sleep and at a reduced rate during awake immobility, consummatory behaviors and grooming (Buzsáki et al., 1983). Several studies have confirmed Buzsáki's prediction of the involvement of slow-wave sleep in the consolidation of hippocampus-dependent memories (Plihal and Born, 1997; Gais and Born, 2004; Peigneux et al., 2004). Furthermore, manipulations designed to enhance some aspects of slow-wave sleep, including the sensory content of neuronal activity, resulted in an improved performance for hippocampus-dependent memory tasks learned before sleep (Marshall et al., 2006; Rasch et al., 2007). In parallel, increases in sharp wave-ripple events have been described after learning in both humans and rats (Axmacher et al., 2008; Eschenko et al., 2008). These results strengthen the hypothesis that the critical attribute of slow-wave sleep for memory consolidation is the presence of sharp wave-ripple events. Further, they suggest that the sharp wave-ripple events that take place during awake behaviors could also have a function in the acquisition, processing, or long-term storage of memory, along with the events occurring during slow-wave sleep (Axmacher et al., 2008).

Reactivation of patterns of awake neuronal activity has been observed during sleep in the hippocampus of rats (Wilson and McNaughton, 1994; Nadasdy et al., 1999) and of humans (Peigneux et al., 2004), and in the bird song system (Dave and Margoliash, 2000). Remarkably, in the hippocampus of the rat, the reactivation of spatial memory patterns has been explicitly observed at the cellular level as temporally ordered sequences of activity of hippocampal neurons. These replay events occur in association with population sharp wave-ripple events, either during

Department of Brain and Cognitive Sciences, The Picower Institute for Learning and Memory, RIKEN-MIT Neuroscience Research Center, Massachusetts Institute of Technology, Cambridge, Massachusetts

Additional Supporting Information may be found in the online version of this article.

Valerie Ego-Stengel is currently at Unité de Neurosciences Intégratives et Computationnelles, Institut Fédératif de Neurobiologie Alfred Fessard, CNRS, Gif-sur-Yvette, France.

Grant sponsors: RIKEN Institute, NIH, The Human Frontier Science Program Organization, Long-Term Fellowship (to V.E.S.); Grant number: RO1 MH061976

*Correspondence to: Valerie Ego-Stengel, Unité de Neurosciences Intégratives et Computationnelles, Institut Fédératif de Neurobiologie Alfred Fessard, CNRS, bâtiment 33, Gif-sur-Yvette, France. E-mail: Valerie.Stengel@unic.cnrs-gif.fr or mwilson@mit.edu

Accepted for publication 12 August 2009

DOI 10.1002/hipo.20707

Published online 8 October 2009 in Wiley InterScience (www.interscience.wiley.com).

sleep (Lee and Wilson, 2002; Ji and Wilson, 2007) or during awake behavior (Foster and Wilson, 2006; Diba and Buzsaki, 2007), and both in forward (Lee and Wilson, 2002; Diba and Buzsaki, 2007; Ji and Wilson, 2007) and reverse order (Foster and Wilson, 2006; Diba and Buzsaki, 2007). As part of his memory formation model, Buzsaki had indeed predicted sharp wave-associated (reverse) replay of sequential cellular activity after training (Buzsaki, 1989).

The present study was designed to specifically test whether these highly structured replay events could be one of the mechanisms of memory consolidation. We used electrical stimulation on afferents to the CA1 region of the hippocampus to locally perturb activity during sharp wave-ripple events. The perturbation was applied daily in rats for 1 h after learning of one spatial navigation task, but not after learning of another similar task. Stimulation did not change the sleep/wake architecture of the ongoing rest period. We measured the behavioral performance of the rats in the two mazes and found impairment for the task that was followed by stimulation relative to the control task. In parallel, we assessed the temporal duration of the effects of stimulation on the neuronal activity by analyzing the LFP, the occurrence of sharp wave-ripple events, and the multi-unit activity recorded through tetrodes in CA1. Neuronal activity was suppressed for several hundreds of milliseconds after each stimulation, which corresponds to the duration of sharp wave-ripple events.

MATERIALS AND METHODS

Tetrode Implantation and Recording

All procedures were approved by the Committee on Animal Care at MIT and followed US NIH guidelines. Six male Long-Evans rats (3–7 months old) were implanted under deep surgical anesthesia (isoflurane 0.3–2%) with two arrays of independently movable recording tetrodes. One array of 2–12 tetrodes was aimed at the right CA1 pyramidal cell layer (coordinates 4.0 posterior to bregma, 2.5 lateral to midline). The tetrodes were advanced to their target position over the course of several weeks. One additional tetrode in the array was left in the white matter above CA1 as a reference for differential recordings. A second array of six tetrodes was targeted to the ventral hippocampal commissure (VHC) for stimulation of CA3 to CA1 axons (coordinates 1.3 posterior to bregma, 0.8 lateral to midline) (Amaral and Witter, 1995). All electrode placements were confirmed with histology of lesions and dye deposits after the end of the recording sessions (Supporting Information Fig. 1). Electromyogram (EMG) recording was achieved through a bipolar electrode inserted in the neck muscle. Both thresholded extracellular action potentials (31 kHz sampling, 600–6,000 Hz filtering) and continuous local field potentials (LFP; 2 kHz sampling, 1–475 Hz filtering) were recorded from each tetrode. For the multiunit analysis, all events crossing the predefined acquisition threshold (61 μ V) were used.

Behavioral tracking was achieved both during run and sleep epochs by two sets of three infrared light-emitting diodes

mounted on the headstage and blinking in alternation with a sampling rate of 30 Hz each.

Electrical Stimulation

We selected one tetrode in CA1, for which the LFP signal exhibited ripple events of large amplitude, for online ripple detection. The LFP was amplified and filtered online in the ripple band by an 8th-order Butterworth lowpass filter at 400 Hz followed by an 8th-order Butterworth highpass filter at 100 Hz (KrohnHite 3384 analog filters, total gain 10,000). A threshold-crossing detector (FHC Window Discriminator) was used to generate TTL pulses when the ripple amplitude exceeded a value adjusted manually by the experimenter on the first experimental day for each rat (0.1 ± 0.02 mV). These pulses triggered isolated stimulation units via a computer-controlled burst generator with a preset 1-ms delay, and an electronic switch dispatching the command to up to six stimulators. On the day before the first recording, we determined the current level applied on tetrodes located in the VHC required to produce an effect, as measured by the appearance of individual action potentials at short latencies (~ 10 ms) on some CA1 recording tetrodes, but below the generation of large population postsynaptic potentials. Some stimulation tetrodes were found to be ineffective and were not used further; histology confirmed that these electrodes were not in the VHC. During recordings, stimulation was applied on 3 to 6 tetrodes with an amplitude of 20–60 μ A. Each stimulus was a burst of two 300- μ s biphasic pulses with a 10-ms interval. These parameters were chosen to mimic a typical two-spike burst of a VHC fiber while avoiding tissue damage (Tehovnik, 1996). A 2-s recovery period was forced after any stimulation burst before the next stimulation could be triggered.

Behavioral Training

Before surgery, animals were food-deprived to 85% of their free-feeding weights. They were pretrained to run repeatedly back and forth from one end to the other on a straight linear track for a few days. Training on the experimental mazes began with the recordings, once the tetrodes were localized in the appropriate structures.

We used two identical four-arm radial mazes arranged in one single large wagon-wheel structure (360 cm outer diameter; width of arms 10 cm; Fig. 1A). The center platform was common to the two mazes. One movable transparent wall on an outer arm and eight transparent doors around the center allowed the selection of a specific configuration for each maze. The rat was initially placed at one end of the trajectory (Start) and had to navigate in the correct arms in order to reach the other end (Finish) and retrieve chocolate sprinkles. The rat had to return to the Start, where it received chocolate sprinkles again, to initiate a new trial. Each recording session began with a one-hour rest period in a separate small box. The rat was then trained 15 min on the first maze, allowed to rest for 1 h, then trained 15 min on the second maze and allowed to rest 1 h again. One maze was chosen as the test maze (T) and the

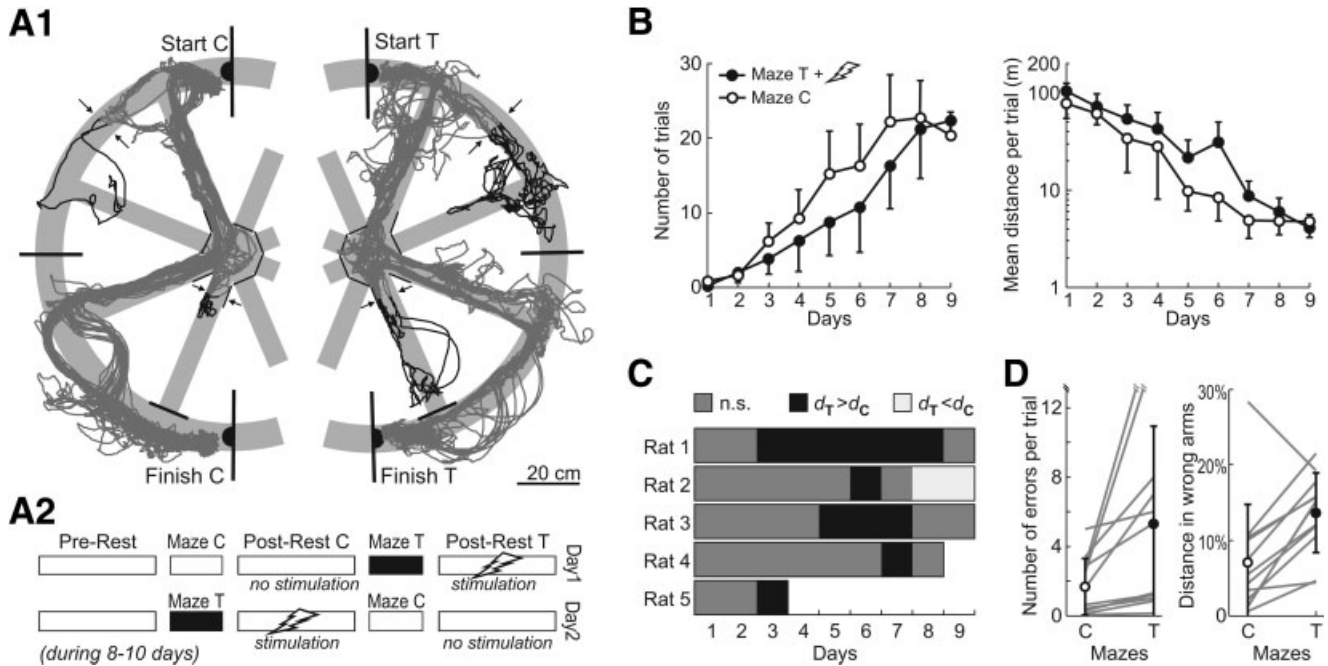


FIGURE 1. Learning is slowed down by ripple disruption during postrest. **A1.** Spatial trajectory of Rat 3 in the two mazes T (test) and C (control) during the sixth day of exploration. The two mazes are created from a unique wagon wheel structure by placing walls and doors on the path; they are separated here for clarity. The trajectory is derived from diodes located on the headstage ~10 cm above the skull. Except to prevent crossing between maze arms, there were no walls on the sides, so that the rat could extend its head well outside of the maze floor (gray areas). In each maze, the rat has to navigate back and forth from the Start point to the Finish point; reward is supplied at both. Exploration of wrong arms is indicated by the black portions of the trajectory. The test maze is chosen randomly for each rat (right/left maze). **A2.** On the first day, the rat initially rests for 1 h. Exploration of the first maze (C or T, randomized across rats) for 15 min is followed by a 1-h rest period; this is repeated for the second maze. Microstimulation is applied during the rest period following maze T. The same sequence is repeated each day for 8–10 days, with alternation of the order of the mazes. **B.** Behavioral deficit in the test maze compared with the control maze. A trial was defined as a complete trajectory from Start to Finish. Left; the number of trials completed per day (\pm standard error of mean, SEM) shows a delay of learning for the test maze compared

with the control maze (ANOVA, day \times maze interaction, $P < 0.009$, five rats). Right; the mean distance per trial (\pm SEM) was longer for the test maze (ANOVA, maze term, $P < 0.025$, and day \times maze interaction, $P < 1.10^{-5}$). **C.** Summary of the days in which the mean distance per trial was similar (gray), longer (black), or shorter (light gray) for the test maze compared with the control maze (two-tailed unpaired Student's *t*-test, $P < 0.05$) for all the rats that learned the task. Rat 5 was terminated on day 4 due to technical problems. For each rat, the first significant difference observed was a longer mean distance in the test maze, and this difference disappeared (and was reversed for Rat 2) at the end of testing. **D.** Increase in trajectory errors accompanying the lengthening of trial distances. Only data from days in which the mean distance per trial was longer in the test maze are plotted (black squares of C). Left; the number of errors per trial (exploration of wrong arms; see black segments in A1) was systematically higher in the test maze compared with the control maze [two-tailed paired Student's *t*-test, $P < 0.03$, $n = 12$; gray lines indicate individual days, black symbols indicate mean \pm standard deviation (SD)]. Right; concomitantly, the fraction of the trajectory traversing the wrong arms was larger for the test maze (two-tailed paired Student's *t*-test, $P < 0.005$, $n = 12$).

other as the control maze (C); the temporal order and physical location of the test maze on the first day was randomized across rats. For each rat, the test and control mazes stayed in the same locations for the rest of training. Stimulation was always applied during the rest period following maze T, and the order of the mazes was alternated from day to day for 8–10 days. On the last planned experimental day, no stimulation was applied. Recordings had to be stopped prematurely after 3 days for one of the rats for technical reasons.

Data Analysis

We categorized sleep states with an automatic sleep scoring algorithm using the neck muscle EMG signal and the same CA1 LFP as used for the online ripple detection. The LFP was

filtered offline with zero-lag by FIR bandpass filters in the delta, theta and ripple bands (1–4, 5–12, 80–250 Hz). Each trace, as well as the EMG signal, was then squared and smoothed with a 10-ms window to obtain the power in each band. In parallel, the velocity of the head was computed from the diode signal to estimate movement. Sleep/wake patterns were classified with a 2-s resolution into three states (Robert et al., 1999; Ji and Wilson, 2007) (Fig. 2A). Wake (high EMG power or nonzero head velocity), rapid eye-movement (REM) sleep (flat EMG power, high θ -to- δ power ratio, low ripple power), and non-REM sleep, which included both clear slow-wave sleep (SWS; low EMG power, low θ -to- δ power ratio, high ripple power) and an intermediate state (INT) consisting mostly of transitions between other states (Gervasoni et al., 2004).

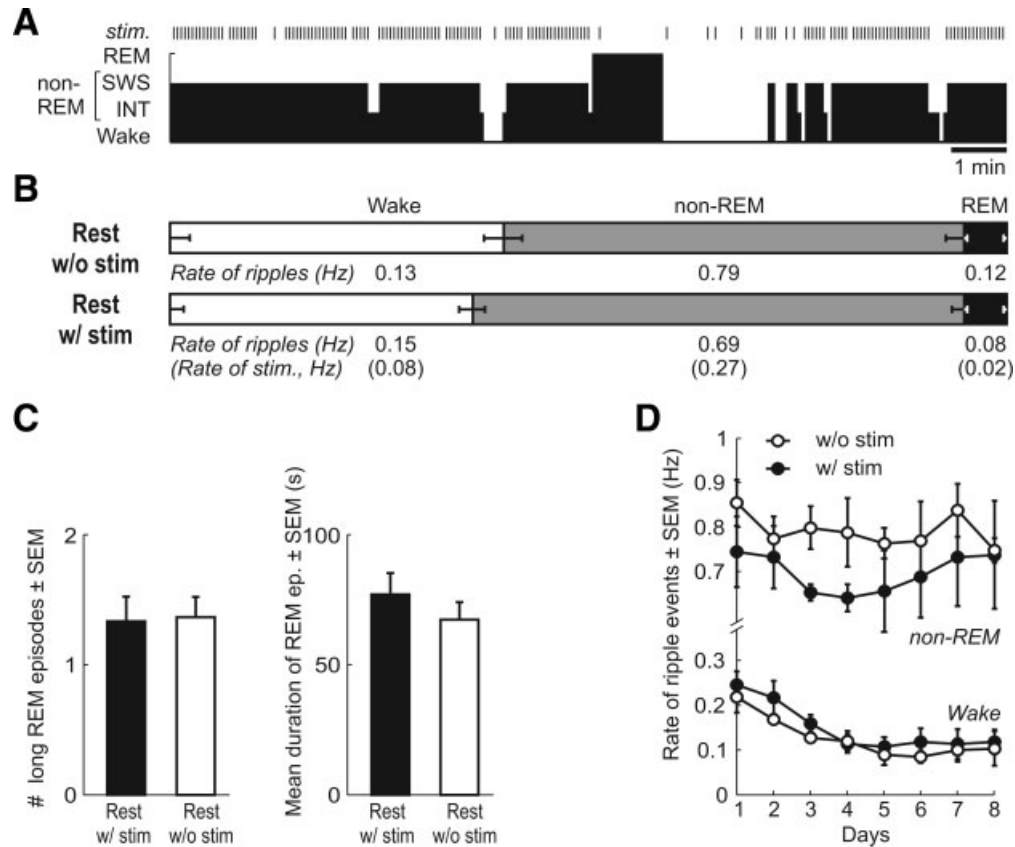


FIGURE 2. The sleep/wake architecture is not modified by stimulation during rest. **A.** Classification into sleep/wake states for a window of 15 minutes of rest with stimulation applied. A normal pattern is observed, consisting of mostly non-REM sleep and, in this case, one episode of REM sleep followed by a Wake period. Bin, 2s. **B.** Fraction of time spent in Wake, non-REM, and REM sleep for the two postrest periods, averaged over all rats and days. Error bars on the inside of each box indicate \pm SEM; everything is relative to the full length of the bar, equal to 1. Below, average rate of ripple events (including the ones interrupted, when applicable) and of stimulation events in each state. The overall structure of the sleep/wake cycle was not affected by the stimulation (two-tailed paired Student's *t*-test, $P > 0.05$, $n = 33$, for each state fraction) and this was true throughout the experiment (ANOVA, Day, Stim, and Day \times Stim interaction terms, $P > 0.05$ for each state fraction). **C.** Number and mean duration of long (>20 s) REM

episodes averaged for the two rest periods. There was no significant difference in these distributions (two-tailed paired Student's *t*-test, $P > 0.8$ and $P > 0.3$, $n = 33$). **D.** Rate of ripple events (including the ones interrupted) as a function of days for the non-REM and Wake states. REM episodes were omitted as they represent a minor fraction of time and have very few ripples (less than one percent of the total). Ripple occurrence in non-REM sleep was quite constant throughout the experiment, whereas in the Wake state, there was a significant drop in the rate of ripple events in the first days, before stabilization at about half the initial value (ANOVA, Days term, $P < 0.0001$ for all data or data restricted to the condition without stimulation). Differences between the conditions with and without stimulation in the non-REM periods are due to suppression of a fraction of ripples by the stimulation (see Fig. 3 and Text).

Ripple events were detected online through hardware in order to initiate stimulation (see above). These triggers were used in the nonstimulation condition as control ripple detections, with which the interrupted ripple events could be compared.

Analysis of the LFP ripple power and of the ripple events around triggers were conducted on the online-filtered ripple signal, even though the causal online filtering necessarily introduces a delay between the raw LFP and the signal coming out of the filtering hardware. We measured this delay as 7 ± 1 ms for all sessions and corrected it by a -7 ms shift of all signals. We did not use the zero-lag FIR filtering for this analysis because the stimulation artifacts sometimes leaked backward in

time by several tens of milliseconds with that method, blurring ripple start estimation.

We applied a standard double-threshold crossing method on the LFP ripple power (Ji and Wilson, 2007) to quantify start, peak, and end points of all ripple events regardless of the online detections. All time points with absolute values larger than a first threshold (mean ripple power + 3SD) were identified as part of a ripple event, and only events with a peak absolute value larger than a second threshold (mean + 10SD) and a duration larger than 30 ms were retained. Gaps smaller than 50 ms were discarded.

Overall, 38 experimental sessions were completed on five rats. We were able to analyze the LFP in both the rest period

with stimulation and the rest period without stimulation in 33 sessions. In the remaining five sessions, either the LFP signal was not available due to technical problems, or no stimulation was applied (last day for the animal).

Behavioral measures were all computer-calculated from the diode-derived trajectories in space and time and were thus blind to condition.

Statistical differences across days and groups (maze T/C, or correspondingly in rest, with/without stimulation) were assessed by a three-way analysis of variance (ANOVA) with Day and Maze (or in rest, Stim) as fixed factors (Zar, 1999). The level of significance was set to 0.05.

All data analysis was conducted using Matlab (MathWorks).

RESULTS

Six rats were implanted with hippocampal recording and stimulation tetrodes, and trained up to 10 days in two identical spatial navigation tasks (Fig. 1A). One rat never explored the mazes and was excluded from the analysis.

Spatial Learning was Impaired by Ripple Disruption During Rest

We first examined the number of Start-to-Finish trajectories completed by each rat on the two mazes as a function of time. On average, the rats learned to navigate the control maze significantly faster than the test maze (Fig. 1B, left). Learning was also quantified by the mean distance per trajectory in the two conditions, which was significantly longer for the test maze (Fig. 1B, right), indicating that the decreased performance was not due to a nonspecific impairment of running. Quantification of the mean time per trajectory led to identical results.

Detailed analysis showed that indeed, for each of the five rats, the first significant difference observed was a longer mean trajectory in the maze associated with stimulation (Fig. 1C). By the end of the experimental sessions, the difference disappeared. Accordingly, the learning curves defined by the number of completed trajectories and the mean distance per trajectory converged in the final days (Fig. 1B).

For the sessions in which we observed significantly longer trajectories, we further quantified the accuracy of navigation in the mazes. Specifically, we counted the number of choice errors, defined as the crossings of virtual boundaries leading to wrong arms of the maze, and measured the fraction of trajectories spent in these wrong arms. For both of these measures, values in the test maze were systematically higher than in the control maze (Fig. 1D, only one exception for the distance measure), confirming that rats were not navigating as efficiently in the test maze for reward retrieval.

We hypothesized that learning could be influenced by two methodological factors: the physical characteristics of each maze, and the order in which the mazes were encountered during each day. The two sides of the custom-made wagon wheel

structure were made as identical as possible; nonetheless, small deviations could exist and the location of each maze in the room (left or right side) was necessarily different. Also, the temporal order in the day (first or second maze exploration) could affect running performance or motivation. We thus performed the same analysis by grouping the learning sessions by physical location or by temporal order during the day (Supporting Information Fig. 2). There was no significant difference in either the number of completed trajectories or the mean trajectory length in these control analyses (ANOVA, Group term and Day \times Group interaction, $P > 0.1$), indicating that the difference in learning found between the control and test mazes is not a trivial consequence of methodological constraints of the experiment.

The control maze exploration sometimes occurred after a 1-h stimulation period, which was never the case for the test maze. Thus, one could argue that the observed behavioral deficit stems in fact from the enhancement by stimulation of the performance in the following control maze in half of the sessions. In order to rule out this possibility, we restricted the analysis to only the first maze explored during each day. For this reduced data set, we still observed a significant difference in the number of completed trajectories and mean trajectory distance between the test and control mazes (ANOVA, Day \times Maze interaction, $P < 0.05$).

We conclude that microstimulation of CA1 afferents triggered by ripple events impairs spatial learning specifically for the task immediately preceding the stimulation.

The Sleep/Wake Architecture was not Modified by Ripple-Triggered Stimulation

The specific aim of our stimulation protocol was to disrupt, during rest, the replay of temporal sequences of hippocampal neuronal activity that had occurred during training. Previous work suggests that this replay occurs during the short sharp-wave-ripple events of both slow-wave sleep and periods of quiet wakefulness. The protocol was thus designed to perturb cellular activity in CA1 during these events, with minimal effects on the global level of neuronal activity or on the sleep/wake architecture.

We analyzed the sequence of Wake, non-REM, and REM sleep states for each 1-h rest period after exploration (Fig. 2A) and compared the results obtained for the rest with stimulation to those obtained for the control rest of the same experimental session, i.e., the same animal and day. This paired analysis established that the fraction of time spent in each of the three states was similar for the two conditions and did not change with time (Fig. 2B). The rest period was always restricted to 1 h within a few minutes (63 ± 3 min), thus this was true for absolute times as well (Supporting Information Fig. 3). Additionally, the number and duration of REM episodes were similar (Fig. 2C), confirming the overall lack of changes in the sleep/wake architecture during stimulation periods.

We also looked at the rate of ripple events in the different states. As expected, it was higher in non-REM sleep (0.79 Hz)

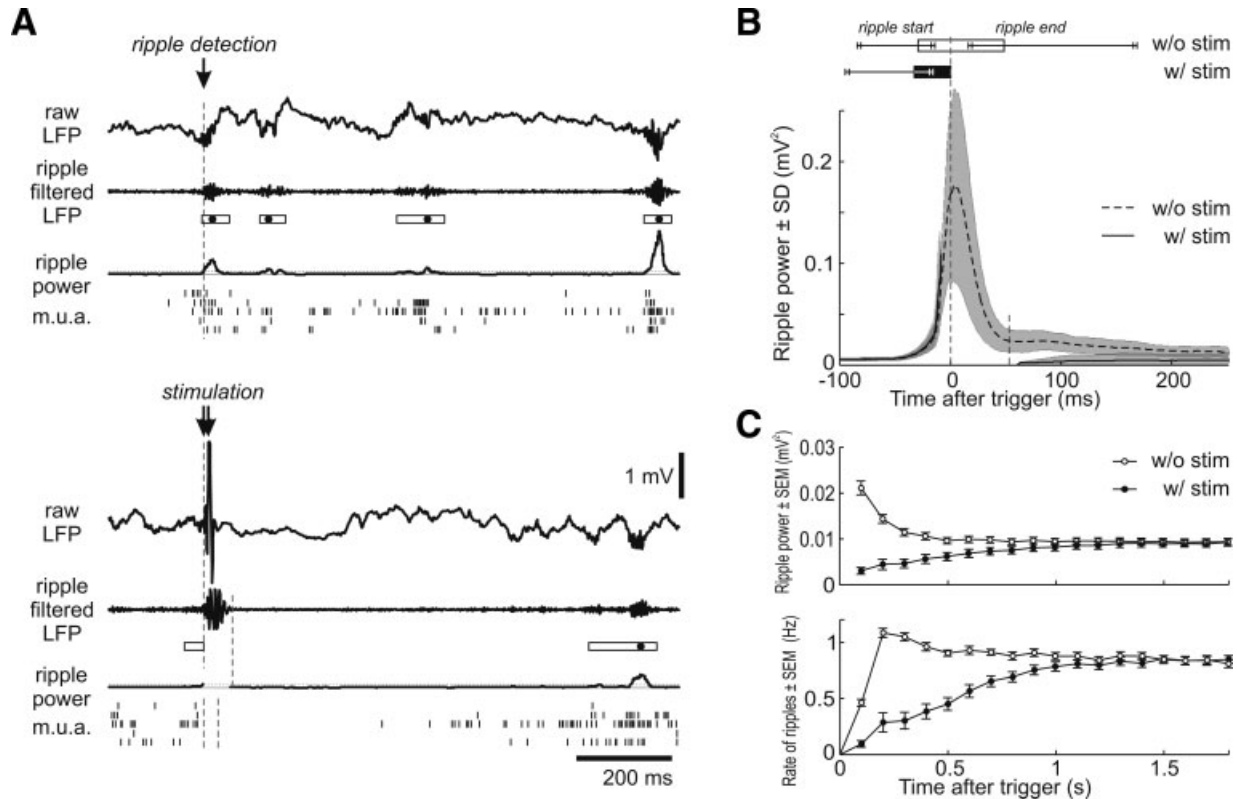


FIGURE 3. Ripple events are interrupted and further ripples suppressed by stimulation. **A.** Top; raw LFP, LFP filtered online in the ripple band (100–400 Hz), power in the ripple band and multiunit activity on five different tetrodes during rest, around the detection of a ripple that would have been stimulated if in a stimulation rest period. The boxes indicate ripples as detected offline by a classic algorithm (see Methods). The inside points correspond to the peaks in ripple power, which had to exceed a threshold (dotted line). Note that there is slight delay (7 ms) introduced by the online-filtering. Bottom; same signals around a stimulation event for the other rest period (same rat and day). The artifact in the raw LFP yields a stereotyped oscillation in the filtered LFP, which contaminates the measurement of the ripple power during a 60-ms period after the stimulation; likewise, the multiunit activity was contaminated during a 30-ms time window (dashed lines). Signal in the ripple band is suppressed for several hundreds of milliseconds, concomitant with a suppression of firing. **B.** Ripple power averaged around stimulations

(solid line) or around ripple detections that would have been stimulated (dashed line). The shaded areas indicate \pm SD across sessions ($n = 33$). Electrical artifacts precluded measurement of ripple power during a 60-ms period after the stimulation, and traces were offset by 7 ms to compensate for the online-filtering delay. Top, box plots showing the duration of ripples detected by the threshold method during a 60-ms period after the stimulation, and traces were offset by 7 ms to compensate for the online-filtering delay. The left of the rectangle box is the median value of the ripple start relative to triggers, and error bars indicate the 10th and 90th percentiles; the right side of the box gives the same values for the ripple end. **C.** Top; Ripple power (\pm SEM) after triggers on a longer time scale. During rest with stimulation, power in the ripple band reaches on average the control value after 1 s. Bottom; number of further ripple events (\pm SEM) developing after triggers. Again, the ripple activity reaches the control value after 1 s. In the nonstimulation condition, there is an excess of new ripples at 200–300 ms above the baseline, illustrating that ripples often come as trains of events.

and was moderately affected by the stimulation (0.69 Hz; Fig. 2B; this includes interrupted ripple events). This difference is not surprising because the stimulation was directly aimed at interrupting and/or suppressing ripple events (see further quantification in Fig. 3), and was relatively constant in time (Fig. 2D). Ripple events in Wake episodes occurring during the 1-h rest periods were much less frequent, but, interestingly, when we looked at the time course of their rate across days, we found a drop during the first 4 days before stabilization at about half the initial value (Fig. 2D). This was true whether stimulation was applied or not. This observation suggests that the occurrence of ripple events during Wake after exploration could be directly regulated by the ongoing behavioral involvement in a spatial learning task.

Hippocampus

Inspection of the stimulation times relative to the sleep/wake structure revealed that most of stimulations occurred during non-REM sleep (84%; Fig. 2A), and a smaller fraction during Wake (15%). Less than 1% of all stimulations occurred during REM, for an average of 687 stimulations per 1-h rest period (see also the rate of stimulation per state in Fig. 2B).

Stimulation Interrupted Ongoing Ripple Events and Suppressed Further Events

Next, we looked in detail at the effect of stimulation on the ongoing ripple events. Double-pulse stimuli of small current amplitude (20–60 μ A) were triggered when the LFP, filtered online by analog hardware in the ripple band (100–400 Hz),

exceeded a preset threshold (see Methods). For comparison, we used the online ripple detections of the control period that “would have been stimulated if in a stimulation period” as triggers for averaging the activity. One control and one stimulation example are given in Figure 3A. The top traces show the raw and filtered LFP before and after online ripple detection in the control rest period. Ripple events were delimited offline by sliding a threshold on the power in the ripple band (rectangles; see Methods). The ripple event started just before the detection and lasted about 50 ms. It was followed shortly after by a second ripple event, and by two additional events in the next second. In contrast, after stimulation (Bottom), the LFP in the ripple band was unusually flat for several hundreds of milliseconds, before multi-unit activity and ripple occurrence eventually resumed.

Averaging over all sessions, we first assessed how the ongoing ripple was altered by stimulation. In Figure 3B, the distributions of ripple start and end times show that stimulation occurred after about one third of the ongoing ripple event, and terminated it, as indicated by the power in the ripple band measured at zero after the electrical artifact period. Analysis on a longer time scale of the ripple power and of the rate of further ripple events confirmed that the network resumed control levels after about 1 s (Fig. 3C). In particular, the tendency of ripple events to come in bursts, indicated by the transient increase in their rate in the first half second of Figure 3C, was blocked by the stimulation protocol.

Neuronal Activity was Suppressed During Several Hundred Milliseconds

We used data from all implanted CA1 recording tetrodes, usually two to five per animal, for quantifying multiunit activity. As shown on the example of Figure 4A, and on the average over all tetrodes and sessions (Fig. 4B, $n = 175$), activity was suppressed for several hundreds of milliseconds after a stimulation, compared to the elevated firing rate following ripple detections in the control period. The baseline level was not affected by the stimulation protocol (two-tailed paired Student's t -test, $P > 0.9$; Pearson correlation coefficient $r = 0.9$), suggesting that the network global activity was only perturbed in localized time windows following stimulations. Furthermore, we looked at the noninterrupted ripple events that occurred in the 2-s refractory periods between two stimulations. The amplitude and profile of activity during these events were identical to those of control ripple events in the nonstimulated rest period. These lack of changes in the network excitability indicate that apart from the transient suppression or ripple-associated activity, the rest period was unaffected by the ongoing stimulation.

DISCUSSION

Spatial navigation in the rat has been used extensively to study the cellular mechanisms underlying memory formation.

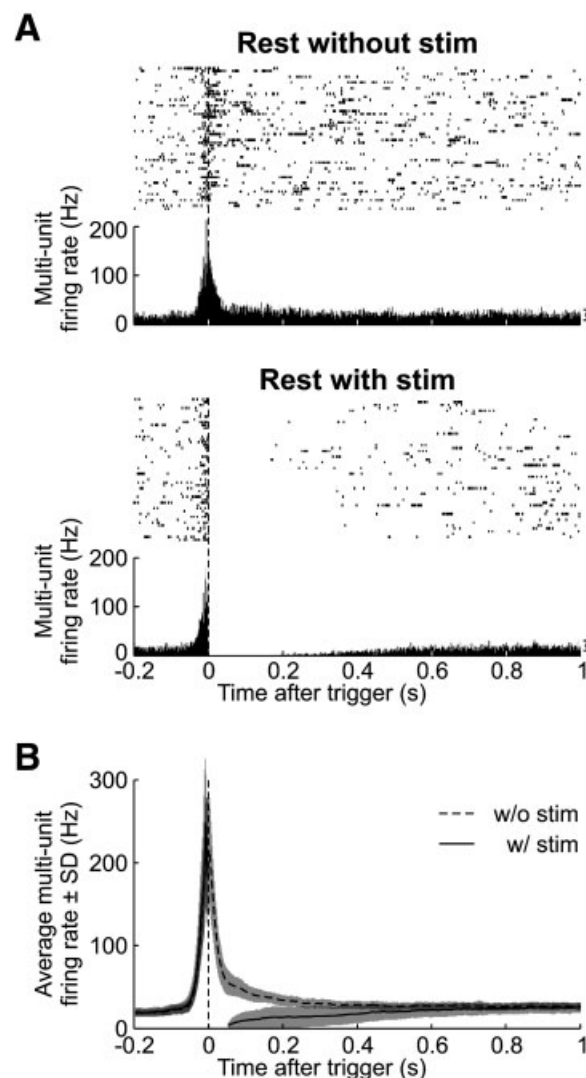


FIGURE 4. The multiunit activity is suppressed by stimulation. **A.** Raster plots and peristimulus time histograms of the multiunit activity recorded by a single tetrode, around ripple detections (Top) and stimulations (Bottom) for the two rest periods of one experimental day. Bin size, 1 ms. The points and error bars on the right indicate the mean spontaneous activity (\pm SD) calculated on the window [1.8–2 s]. Only 50 trials, picked at random and sorted by time, are illustrated in each raster plot, out of 736 (Top) and 853 (Bottom). **B.** Average multiunit activity around stimulations (solid line) or around ripple detections that would have been stimulated (dashed line). Bin size, 5 ms. The shaded areas indicate \pm SD across sessions and tetrodes ($n = 175$). Unsorted electrical artifacts contaminated the activity during a 30-ms period after the stimulation. Multiunit activity was suppressed for several hundred milliseconds by the stimulation.

We designed a task which can be viewed as a modified version of the +maze, known to be hippocampus-dependent (Ferbin-teanu and Shapiro, 2003) and similar to the reference memory versions of the Morris water maze (Morris et al., 1982) or the 8-arm radial maze (Olton et al., 1978). The hypothesis underlying our protocol design is that by disrupting the ripple-associated activity after exploration, we are interfering with core

mechanisms of memory formation. One crucial aspect is that the disruption of neuronal activity should be restricted to patterns representing the maze immediately explored, and not the other maze. Thus, we sought to minimize the putative overlap in the two neuronal representations by eliminating a possible generalization from one maze to the other. The arrangement of the two mazes symmetrically in one large structure removed ambiguity as to what maze the animal was in at each time.

Many studies investigating the role of sleep in learning used sleep deprivation protocols, sometimes restricted to a specific sleep stage (Smith, 1995; Walker and Stickgold, 2004). Although they established a clear link between sleep states and consolidation of some forms of memory, it remains largely unknown what characteristics of sleep are important. Our protocol was specifically designed to target the role of hippocampal ripple-associated activity. To this end, we used brief pulses of low amplitude currents (20–60 μ A) on fine electrodes (tetrodes) so that the disruption would be both localized temporally and spatially. Also, we imposed a minimal 2-s recovery interval between stimulations. Our manipulation was thus very mild compared to that used by Shatskikh and collaborators (Shatskikh et al., 2006), who found spatial learning impairment after induction of interictal spikes, a manifestation of epileptic activity known to perturb the network on a long time scale. Importantly, in our experiments, we found no change in the sequence of sleep/wake states and in the excitability of the network, indicating that the overall brain activity was modestly affected.

Individual sharp wave-ripple events are commonly described to last 50–120 ms, and our recordings agree with this. We estimated that stimulation interrupted ongoing ripple events after about one third of their total duration. More importantly, these events have been known to occur in bursts, typically two to five events close in time (O'Keefe and Nadel, 1978; Buzsaki et al., 1983) (Fig. 3C). Recent observations demonstrate that replay of CA1 activity corresponding to one trajectory can span multiple ripple events, and that typical replay durations after exploration of a long track are in the range of 200–700 ms (Ji and Wilson, 2007). These values correspond to the time of recovery that we observed in the network after stimulation. These results suggest that despite the residual beginnings of ripple events that subsided in our experiments, for the most part the replay activity was probably abolished, and only very short behavioral sequences expressed.

The impairment of memory consolidation by ripple event disruption was only moderate. First, significant differences between the control and test mazes performances were only detected on Day 3 and later (Figs. 1B,C). Given that the first posttraining rest period is often thought to be crucial for sleep-dependent memory consolidation (Smith, 1995), it could have been expected that performance levels would start differentiating on the first day after the first rest stimulation, that is on Day 2 of the protocol. We hypothesize that because the task is fairly difficult, the poor levels of acquisition after the first day are not sufficient to induce strong posttraining behavioral changes and detectable differences in the next performance

assessment. This is in line with experiments in rats showing that when training was distributed over days, the resulting changes in posttraining sleep were distinct from those occurring after massed training (Smith et al., 1980; Smith, 1985).

Second, the learning impairment was restricted in time. The learning curves for the stimulation and control conditions converged by the final experimental day. The partial blockade of memory formation could thus be overcome with additional days of training. One possible explanation would be that the stimulation protocol was only applied during 1 h after exploration. Memory consolidation could take place already during immobility in the exploration period (Foster and Wilson, 2006; Diba and Buzsaki, 2007), and additionally in the 20 h separating the end of one experimental session from the beginning of the next. Moreover, we restricted stimulation frequency to 0.5 Hz so that probable replay occurred during residual ripple events between two successive stimulations and could underlie some memory consolidation for the test maze. Accumulation over many days of these remaining opportunities for memory consolidation would enable performance to eventually reach that of control animals. Note that because the VHC contains both fibers from right CA3 to left CA1 and fibers from left CA3 to right CA1 (Wyss et al., 1980; Adelman et al., 1996), and because we sent currents through several tetrodes simultaneously, it is most likely that both hippocampi were stimulated over a large area, and we cannot attribute the moderate size of the impairment to a unilateral or local effect.

We did not attempt to distinguish online ripple events occurring during slow-wave sleep from those occurring during the awake state. We cannot exclude the possibility that only one type of ripple events participates in memory consolidation. In fact, our data revealed a different time course of the rate of these two subsets during sleep, arguing for possible functional differences. Ripple events during the awake state were twice as numerous in the first day of training compared to the last days. This observation is compatible with a specific involvement of sharp wave-ripple events, and maybe particularly those of the awake state, in consolidation of behavioral learning. This result agrees with a recent report of ripple events increase after training in the rat (Eschenko et al., 2008), although these authors focused on slow-wave sleep associated events. Interestingly, in the human, a similar increase in postlearning ripple events has been found, but specifically during awake resting periods (Axmacher et al., 2008).

By disrupting the ripple events and demonstrating an impairment in learning, we establish a causal link between neuronal activity known to contain replay and memory consolidation. The question of how exactly replay would participate in memory formation remains, however, open. Several mutually compatible hypotheses have been brought forward. Replay events are one manifestation of a more general phenomenon, which is the existence of internally generated structured activity in the hippocampus (Gelbard-Sagiv et al., 2008; Pastalkova et al., 2008). These bouts of activity, including those generated for explicit information retrieval, probably contribute to restructuring of memory representations for increased

behavioral performance, beyond a role of pure memory consolidation (Hennevin et al., 2007). Given the known level of plasticity of representations in the adult brain, reactivation of specific memories could be necessary to maintain adequate representations in the face of an ever-changing physical network implementation (Kali and Dayan, 2004). From this point of view, replay events should naturally be privileged times for synaptic plasticity. Indeed, the temporal compression brings signals in the range of known synaptic plasticity rules. It has been recently suggested that the population bursts of sharp wave-ripples serve to desynchronize neurons through STDP rules, thus preventing blowup of excitation in the hippocampal network and selectively erasing some memories but not others (Lubenov and Siapas, 2008). In particular, this mechanism would gradually weaken hippocampal representations of memories.

Sharp wave-ripple events have specifically been proposed to underlie the gradual transfer of memories from hippocampus to cortex, providing active communication between these structures during rest periods (Buzsaki, 1996). In support of this hypothesis, sharp wave-ripple events in the hippocampus have been shown to occur in close temporal proximity to neocortical spindles (Siapas and Wilson, 1998) and neocortical transitions from down to up states (Battaglia et al., 2004). It would indeed be interesting to investigate whether ripple disruption during rest and the resulting memory impairment are accompanied by a change in neocortical spindles or up states. Moreover, it has recently been suggested that whereas many replay events are generated in the hippocampus, only those relevant for the consolidation of behaviorally significant memories would be transferred to the entorhinal cortex (EC) and further cortices (Axmacher et al., 2008), where they could trigger synaptic plasticity. This suggests a more subtle manipulation in which only the replay events for which the hippocampus and cortex are actively interacting would be disrupted. Future studies will help elucidate whether the function of neuronal replay is predominantly to regulate the hippocampal network itself, or to enable information transfer to the neocortex for long-term memory consolidation of events meeting behavioral performance criteria, or both.

Acknowledgments

The authors thank Arielle Tambini for outstanding technical help during preliminary experiments, Tom Davidson for help with the 3D design of implant parts, Paul Galloux for technical computer assistance, and members of the Wilson lab and UNIC for numerous discussions. V.E.S. is particularly grateful to Daniel Shulz for unfailing support.

REFERENCES

Adelmann G, Deller T, Frotscher M. 1996. Organization of identified fiber tracts in the rat fimbria-fornix: An anterograde tracing and electron microscopic study. *Anat Embryol (Berl)* 193:481–493.

Amaral DG, Witter MP. 1995. Hippocampal formation. In: Paxinos G, editor. *The Rat Nervous System*, 2nd ed. San Diego, CA: Academic Press. pp 443–493.

Axmacher N, Elger CE, Fell J. 2008. Ripples in the medial temporal lobe are relevant for human memory consolidation. *Brain* 131:1806–1817.

Battaglia FP, Sutherland GR, McNaughton BL. 2004. Hippocampal sharp wave bursts coincide with neocortical “up-state” transitions. *Learn Mem* 11:697–704.

Buzsaki G. 1986. Hippocampal sharp waves: Their origin and significance. *Brain Res* 398:242–252.

Buzsaki G. 1989. Two-stage model of memory trace formation: A role for “noisy” brain states. *Neuroscience* 31:551–570.

Buzsaki G. 1996. The hippocampo-neocortical dialogue. *Cereb Cortex* 6:81–92.

Buzsaki G, Leung LW, Vanderwolf CH. 1983. Cellular bases of hippocampal EEG in the behaving rat. *Brain Res* 287:139–171.

Dave AS, Margoliash D. 2000. Song replay during sleep and computational rules for sensorimotor vocal learning. *Science* 290:812–816.

Diba K, Buzsaki G. 2007. Forward and reverse hippocampal place-cell sequences during ripples. *Nat Neurosci* 10:1241–1242.

Eschenko O, Ramadan W, Molle M, Born J, Sara SJ. 2008. Sustained increase in hippocampal sharp-wave ripple activity during slow-wave sleep after learning. *Learn Mem* 15:222–228.

Ferbinteanu J, Shapiro ML. 2003. Prospective and retrospective memory coding in the hippocampus. *Neuron* 40:1227–1239.

Foster DJ, Wilson MA. 2006. Reverse replay of behavioural sequences in hippocampal place cells during the awake state. *Nature* 440:680–683.

Gais S, Born J. 2004. Declarative memory consolidation: Mechanisms acting during human sleep. *Learn Mem* 11:679–685.

Gelbard-Sagiv H, Mukamel R, Harel M, Malach R, Fried I. 2008. Internally generated reactivation of single neurons in human hippocampus during free recall. *Science* 322:96–101.

Gervasoni D, Lin SC, Ribeiro S, Soares ES, Pantoja J, Nicolelis MA. 2004. Global forebrain dynamics predict rat behavioral states and their transitions. *J Neurosci* 24:11137–11147.

Hennevin E, Huetz C, Edeline JM. 2007. Neural representations during sleep: From sensory processing to memory traces. *Neurobiol Learn Mem* 87:416–440.

Ji D, Wilson MA. 2007. Coordinated memory replay in the visual cortex and hippocampus during sleep. *Nat Neurosci* 10:100–107.

Kali S, Dayan P. 2004. Off-line replay maintains declarative memories in a model of hippocampal-neocortical interactions. *Nat Neurosci* 7:286–294.

Lee AK, Wilson MA. 2002. Memory of sequential experience in the hippocampus during slow wave sleep. *Neuron* 36:1183–1194.

Lubenov EV, Siapas AG. 2008. Decoupling through synchrony in neuronal circuits with propagation delays. *Neuron* 58:118–131.

Marshall L, Helgadottir H, Molle M, Born J. 2006. Boosting slow oscillations during sleep potentiates memory. *Nature* 444:610–613.

Morris RG, Garrud P, Rawlins JN, O’Keefe J. 1982. Place navigation impaired in rats with hippocampal lesions. *Nature* 297:681–683.

Nadasdy Z, Hirase H, Czurko A, Csicsvari J, Buzsaki G. 1999. Replay and time compression of recurring spike sequences in the hippocampus. *J Neurosci* 19:9497–9507.

O’Keefe J, Nadel L. 1978. *The Hippocampus as a Cognitive Map*. Oxford, UK: Oxford University Press.

Olton DS, Walker JA, Gage FH. 1978. Hippocampal connections and spatial discrimination. *Brain Res* 139:295–308.

Pastalkova E, Itskov V, Amarasingham A, Buzsaki G. 2008. Internally generated cell assembly sequences in the rat hippocampus. *Science* 321:1322–1327.

Peigneux P, Laureys S, Fuchs S, Collette F, Perrin F, Reggers J, Phillips C, Degueldre C, Del Fiore G, Aerts J, Luxen A, Maquet P. 2004. Are spatial memories strengthened in the human hippocampus during slow wave sleep? *Neuron* 44:535–545.

- Plihal W, Born J. 1997. Effects of early and late nocturnal sleep on declarative and procedural memory. *J Cognit Neurosci* 9:534–547.
- Rasch B, Buchel C, Gais S, Born J. 2007. Odor cues during slow-wave sleep prompt declarative memory consolidation. *Science* 315:1426–1429.
- Robert C, Guilpin C, Limoge A. 1999. Automated sleep staging systems in rats. *J Neurosci Methods* 88:111–122.
- Shatskikh TN, Raghavendra M, Zhao Q, Cui Z, Holmes GL. 2006. Electrical induction of spikes in the hippocampus impairs recognition capacity and spatial memory in rats. *Epilepsy Behav* 9:549–556.
- Siapas AG, Wilson MA. 1998. Coordinated interactions between hippocampal ripples and cortical spindles during slow-wave sleep. *Neuron* 21:1123–1128.
- Smith C. 1985. Sleep states and learning: A review of the animal literature. *Neurosci Biobehav Rev* 9:157–168.
- Smith C. 1995. Sleep states and memory processes. *Behav Brain Res* 69:137–145.
- Smith C, Young J, Young W. 1980. Prolonged increases in paradoxical sleep during and after avoidance-task acquisition. *Sleep* 3:67–81.
- Squire LR, Stark CE, Clark RE. 2004. The medial temporal lobe. *Annu Rev Neurosci* 27:279–306.
- Tehovnik EJ. 1996. Electrical stimulation of neural tissue to evoke behavioral responses. *J Neurosci Methods* 65:1–17.
- Walker MP, Stickgold R. 2004. Sleep-dependent learning and memory consolidation. *Neuron* 44:121–133.
- Wilson MA, McNaughton BL. 1994. Reactivation of hippocampal ensemble memories during sleep. *Science* 265:676–679.
- Wyss JM, Swanson LW, Cowan WM. 1980. The organization of the fimbria, dorsal fornix and ventral hippocampal commissure in the rat. *Anat Embryol (Berl)* 158:303–316.
- Zar JH. 1999. *Biostatistical Analysis*. Upper Saddle River, NJ: Prentice Hall.